Magnetic domain observations in a FeCo-based nanocrystalline alloy by Lorentz microscopy

Jianguo Long,[a] Yueling Qin, Tom Nuhfer, M. De Graef, D. E. Laughlin, and M. E. McHenry
Materials Science and Engineering, Carnegie Mellon University, Pittsburgh, Pennsylvania 15213

(Presented on 10 January 2007; received 31 October 2006; accepted 24 January 2007; published online 8 May 2007)

Lorentz microscopy was used to investigate the domain structure in an $(Fe_{0.5}Co_{0.5})_{80}Nb_4B_{13}Ge_2Cu_1$ alloy annealed at 500, 550, and 610 °C, respectively, for 1 h. The average grain size d, observed by conventional transmission electron microscopy, is 10 nm for the alloy annealed at 500 °C, 18 nm for 550 °C, and 90 nm for 610 °C. The domain structure of sample annealed at 500 °C exhibits few pinning sites and large domains, which correlate with the low coercivity and good soft magnetic properties. More pinning sites and smaller domains are observed in the sample annealed at 550 °C. In the sample annealed at 610 °C, the domain walls are observed to be localized at the grain boundaries and the domains include several grains. It therefore appears that the grain boundaries act as effective pinning sites in this sample. As expected, domain walls in the 610 °C sample are less mobile in small applied fields than in the 500 and 550 °C samples. This result is consistent with coercivity measurement and the random anisotropy model commonly used to rationalize the coercivity dependence on average grain size in these alloys. © *2007 American Institute of Physics*.
[DOI: 10.1063/1.2714309]

INTRODUCTION

In the past several decades, nanocrystalline soft magnetic materials have received increased attention because of their excellent soft magnetic properties. Most of these nanocrystalline soft magnetic alloys are prepared by primary crystallization of amorphous precursors; thus the resultant microstructure contains a considerable amount of the residual amorphous phase. For example, in nanocrystalline soft magnetic alloys Fe–Nb–B–Si–Cu,[1] Fe–M–B (M=Nb, Zr, Hf, etc.),[2] and Fe–Co–Zr–B–Cu,[3,4] it has been reported that the best soft magnetic properties are achieved under conditions where a nanocrystalline phase is surrounded by the amorphous phase resulting in the so-called nanocomposites. In order to understand the origin of the soft magnetic properties of these materials, it is necessary to investigate the correlations between the microstructure and the magnetic domain structure.

Lorentz microscopy is a technique for the direct observation of magnetic domain structures. In classical Lorentz microscopy, the electron experiences a deflection force proportional to both the magnetic induction B and the electron velocity. The deflection angle θ_L is given by[5]

$$\theta_L = \frac{e\lambda}{h} B_\perp t, \tag{1}$$

where λ is the relativistic electron wavelength, $B_\perp$ is the magnetic induction component normal to the electron trajectory, and t is the local sample thickness. θ_L is typically in the range of tens of microradians. The deflection of the electrons can be used to obtain images in Foucault and Fresnel modes. Lorentz microscopy has been previously used to study nanocomposite soft magnetic HITPERM alloys.[6]

Although magnetic domain structures in thin specimens are different from those in bulk specimens, the observation of magnetic domain structures of the thin specimens can still yield valuable information that can be used to further understand the magnetic properties of bulk materials. Here, we present the domain structure analysis of FeCo-based nanocrystalline soft magnetic materials prepared through annealing at different temperatures as studied by Lorentz microscopy.

EXPERIMENT

Amorphous ribbon, ~30 μm thick and ~3 mm wide, of nominal composition $(Fe_{0.5}Co_{0.5})_{80}Nb_4B_{13}Ge_2Cu_1$ was prepared by single roller melt spinning. The alloy was induction melted in a quartz crucible and cast with in argon onto a copper wheel rotating at ~50 m/s in a vacuum chamber. Amorphous samples were subsequently crystallized by sealing them in evacuated silica tubes, placing them in a preheated furnace at prescribed temperatures for 1 h and then water quenched to room temperature.

X-ray diffraction (XRD) with Cu $K\alpha$ radiation was used to study the structural and phase evolution as a function of the annealing temperature. A vibrating sample magnetometer (VSM) was used to measure the coercivity H_c. A JEOL JEM2000 conventional transmission electron microscope operated at 200 keV was employed to characterize the microstructure. High-resolution transimission electron microscope (HRTEM) and Lorentz microscope images were obtained using a Philips TECNAI-F20 transmission electron microscope with energy dispersive spectroscopy (EDS) capability. TEM samples were prepared by ion milling.

[a]Electronic mail: jianguol@andrew.cmu.edu

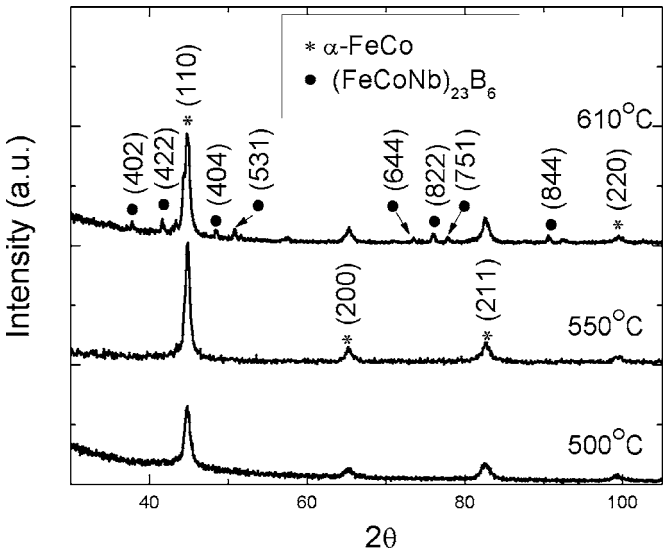

FIG. 1. X-ray pattern for samples isothermally annealed at indicated temperature for 1 h.

RESULT AND DISCUSSION

The structural evolution as a function of annealing temperatures as determined by XRD is shown in Fig. 1. The onset temperature of primary crystallization of the sample was determined to be ~405 °C by differential scanning calorimetry (DSC). The diffraction pattern for the specimen annealed at 500 °C for 1 h revealed primary crystallization of an α-FeCo phase. The HRTEM observation also confirmed the nanocrystalline α-FeCo phase to be embedded in an amorphous matrix (Fig. 2). With increasing annealing temperature, the volume fraction of the nanocrystalline α-FeCo phase increased due subsequent growth. When the sample was annealed at 610 °C for 1 h, secondary crystallization of an $(FeCoNb)_{23}B_6$ phase was observed (Fig. 1).

Figure 3 shows bright field images for samples annealed at 500, 550, and 610 °C, respectively, for 1 h. To determine the grain size, the dark field images corresponding to the bright field images shown in Figs. 3(a)–3(c) were employed. In calculating average grain size, an implicit assumption of

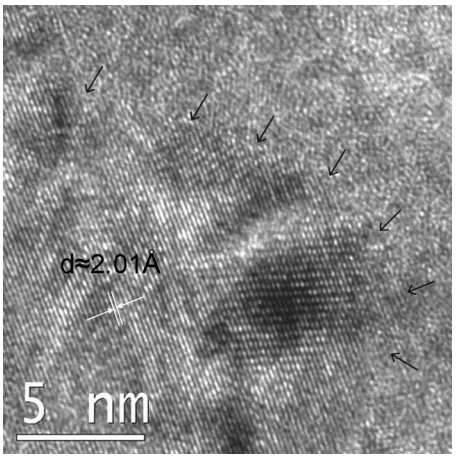

FIG. 2. High-resolution TEM image for sample annealed at 500 °C for an hour. α-FeCo (110) planes are shown, and arrows indicate the boundary between the amorphous matrix and the nanoparticle.

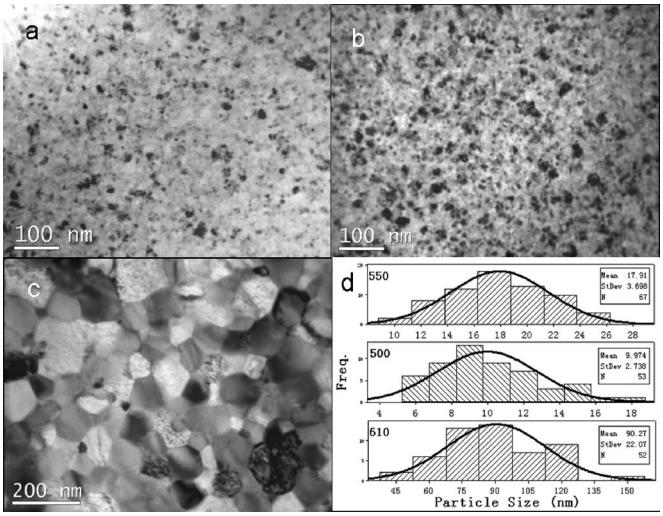

FIG. 3. Bright field TEM images for sample annealed at (a) 500 °C, (b) 550 °C, and (c) 610 °C for 1 h. (d) Grain size distribution.

spherical grains was employed and the diameter for each grain was assigned to be the longest line length contained within. A grain size distribution, thus determined, is shown in Fig. 3(d). The average grain size estimated by fitting the size distribution using a Lorentzian function was about 10 nm for 500 °C, 18 nm for 550 °C, and 90 nm for 610 °C.

Figures 4 and 5 show Lorentz microscopy images of the $(Fe_{0.5}Co_{0.5})_{80}Nb_4B_{13}Ge_2Cu_1$ alloy having undergone various heat treatments. The Lorentz microscopy images were observed in the Fresnel mode. The Lorentz microscopy image of the specimen annealed at 500 °C for 1 h is shown in Fig. 4(a) with domain walls evident as white and black lines. Figure 4(b) shows the domain pattern of a selected area (dashed square region) from Fig. 4(a) after defocusing in the opposite direction. The bright line in Fig. 4(a) is seen to reverse its contrast in Fig. 4(b). The width of domain walls (δ_w) can be measured from the width of the divergent wall image (w) as a function of defocus Δf and extrapolating to zero Δf:[7]

$$w(\Delta f) = \delta_w + \Delta f \Phi(\Delta f). \tag{2}$$

Equation (2) was used to estimate the domain wall width of the specimen annealed at 500 °C for 1 h. The domain wall

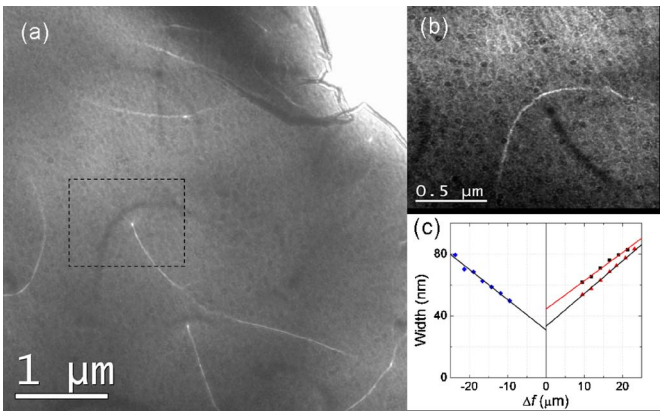

FIG. 4. (Color online) Lorentz microscope image of sample annealed at 500 °C.

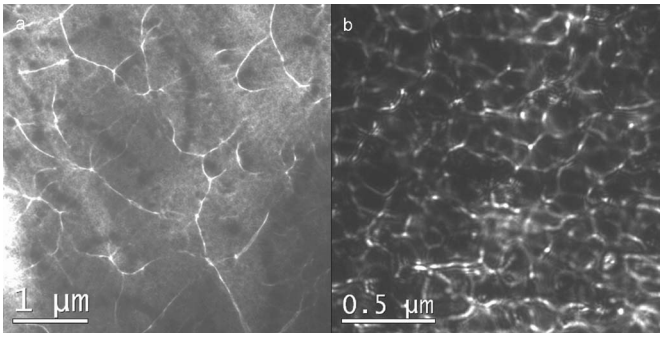

FIG. 5. Lorentz microscope image of sample annealed at (a) 550 °C and (b) 610 °C.

width was determined to be ~50 nm in the specimen annealed at 500 °C which has an average grain size of 10 nm.[7]

Figure 5(a) shows the Lorentz microscopy image of the specimen annealed at 550 °C for 1 h. Compared with the Lorentz microscopy image of Fig. 4, Fig. 5(a) exhibits smaller domains and many more domain wall pinning sites. The domain structure at 500 °C exhibits relatively few pinning sites and large domains, which correlate well with a low coercivity and good soft magnetic properties. Relatively more pinning sites and smaller domains were observed in a sample annealed at 550 °C, indicating that domains in the sample annealed at 550 °C should be pinned more effectively. In the sample annealed at 610 °C, the domain walls are only observed in grain boundary and a domain includes several grains, as shown in Fig. 5(b). It therefore appears that the grain boundary plays a role in pinning the walls. The coercivities measured by VSM were 1.6 Oe for 500 °C, 3.1 Oe for 550 °C, and 11.5 Oe for 610 °C, respectively.

According to the Herzer model,[8,9] when grain size is much smaller than the ferromagnetic exchange length, the magnetocrystalline anisotropy of the grains (with randomly oriented easy axes) is averaged and therefore domain walls are not pinned by grain boundaries. For larger grain sizes, the statistical averaging of the magnetocrystalline anisotropy energy is diminished and walls are pinned more effectively as a result. From Figs. 4 and 5, it is clear that domain walls are more strongly pinned in the intergranular region for the samples treated at higher annealing temperatures. This pinning is correlated with the larger effective grain size.

CONCLUSION

The presence of domain wall pinning sites at grain boundaries was observed in nanocrystalline soft magnetic alloy with nominal composition $(Fe_{0.5}Co_{0.5})_{80}Nb_4B_{13}Ge_2Cu_1$ after annealing at 610 °C for 1 h. The domain size and pinning sites are strongly dependent on grain size. This is consistent with coercivity measurement and the Herzer model predictions. At the finest sizes of the nanocrystals ($d < \sim 10$ nm), the material behaves as a true nanocomposite while at larger sizes the walls become localized in the intergranular region ($d \sim 90$ nm).

ACKNOWLEDGMENTS

This work was supported by National Science Foundation DMR-0406220. This work was also supported in part by the Army Research Laboratory and was accomplished under Cooperative Agreement No. W911NF-04-2-0017. The views and conclusions contained in this document are those of the authors and should not be interpreted as representing the official policies, either expressed or implied, of the Army Research Laboratory or the U.S. Government.

[1] Y. Yoshizawa, S. Oguma, and K. Yamauchi, J. Appl. Phys. **64**, 6044 (1988).
[2] K. Suzuki, N. Ktaoka, A. Inoue, A. Makino, and T. Masumoto, Mater. Trans., JIM **31**, 743 (1990).
[3] M. A. Willard, D. E. Laughlin, M. E. McHenry, D. Thoma, K. Sickafus, J. O. Cross, and V. G. Harris, J. Appl. Phys. **84**, 6773 (1998).
[4] M. E. McHenry, M. A. Willard, and D. E. Laughlin, Prog. Mater. Sci. **44**, 291 (1999).
[5] M. De Graef, *Experimental Methods in the Physical Sciences* (Academic, 2000), Vol. 36, p. 27–67.
[6] M. De Graef, M. Willard, D. E. Laughlin, and M. E. McHenry, IEEE Trans. Magn. **37**, 2243 (2001).
[7] H. Gong and J. N. Chapman, J. Magn. Magn. Mater. **67**, 4 (1987).
[8] G. Herzer, IEEE Trans. Magn. **25**, 3327 (1989).
[9] G. Herzer, IEEE Trans. Magn. **26**, 1397 (1990).